

# Unveiling the $a_0(1710)$ nature in the process $J/\psi \rightarrow \bar{K}^0 K^+ \rho^-$

Yan Ding,<sup>1</sup> En Wang,<sup>1,2,\*</sup> De-Min Li,<sup>1,†</sup> Li-Sheng Geng,<sup>3,4,5,6,‡</sup> and Ju-Jun Xie<sup>6,7,8,§</sup>

<sup>1</sup>*School of Physics and Microelectronics, Zhengzhou University, Zhengzhou, Henan 450001, China*

<sup>2</sup>*Guangxi Key Laboratory of Nuclear Physics and Nuclear Technology, Guangxi Normal University, Guilin 541004, China*

<sup>3</sup>*School of Physics, Beihang University, Beijing 102206, China*

<sup>4</sup>*Beijing Key Laboratory of Advanced Nuclear Materials and Physics, Beihang University, Beijing, 102206, China*

<sup>5</sup>*Peng Huanwu Collaborative Center for Research and Education, Beihang University, Beijing 100191, China*

<sup>6</sup>*Southern Center for Nuclear-Science Theory (SCNT), Institute of Modern Physics, Chinese Academy of Sciences, Huizhou 516000, Guangdong Province, China*

<sup>7</sup>*Institute of Modern Physics, Chinese Academy of Sciences, Lanzhou 730000, China*

<sup>8</sup>*School of Nuclear Sciences and Technology, University of Chinese Academy of Sciences, Beijing 101408, China*

(Dated: February 1, 2024)

We have investigated the process  $J/\psi \rightarrow \bar{K}^0 K^+ \rho^-$  by taking into account the  $S$ -wave  $K^* \bar{K}^*$ ,  $\rho\omega$ , and  $\rho\phi$  final state interactions within the unitary coupled-channel approach, where the scalar meson  $a_0(1710)$  is dynamically generated. In addition, the contributions from the intermediate resonances  $K_1(1270)^- (\rightarrow \bar{K}^0 \rho^-)$  and  $K_1(1270)^0 (\rightarrow K^+ \rho^-)$  are also considered. We find a significant peak structure around 1.8 GeV, associated to the  $a_0(1710)$ , in the  $\bar{K}^0 K^+$  invariant mass distribution, and the clear peaks of the  $K_1(1270)$  in the  $\bar{K}^0 \rho^-$  and  $K^+ \rho^-$  invariant mass distributions. A precise measurement of this process by the BESIII and BelleII Collaborations and at the planed super tau charm facility in the future could shed light on the nature of  $a_0(1710)$ .

PACS numbers:

## I. INTRODUCTION

In the last two decades, it has been accumulated experimentally many states whose properties can not be well described by the  $q\bar{q}$  mesons and the  $qqq$  baryons within the conventional quark model. Some exotic explanations are proposed for their nature, such as tetraquark, pentaquark, hybrid, glueball, kinematic effects, and the mixing of different components. It is difficult to distinguish between those explanations, especially for states with the quantum numbers the conventional quark model allows.

Recently, the *BABAR* Collaboration reported the scalar resonance  $a_0(1710)$  in the  $\pi^\pm \eta$  invariant mass spectrum of the process  $\eta_c \rightarrow \eta \pi^+ \pi^-$  [1]. The  $a_0(1710)$  state was also observed by the BESIII Collaboration in the  $K_S^0 K_S^0$  invariant mass spectrum of the process  $D_s^+ \rightarrow K_S^0 K_S^0 \pi^+$  [2] and in the  $K_S^0 K^+$  invariant mass spectrum of the process  $D_s^+ \rightarrow K_S^0 K^+ \pi^0$  [3]. We have tabulated the experimental masses and widths of  $a_0(1710)$  in Table I. It should be noted that, in Ref. [2], BESIII did not distinguish between the  $a_0(1710)$  and  $f_0(1710)$  in the process  $D_s^+ \rightarrow K_S^0 K_S^0 \pi^+$ , and denoted the combined state as  $S(1710)$ , while in Ref. [3] the  $a_0(1710)$  was renamed as  $a_0(1817)$  because of the different fitted Breit-Wigner mass of this state.

Before the observation of  $a_0(1710)$ , there have been many theoretical studies about the  $a_0(1710)$  and its

TABLE I: Experimental measurements on the mass [ $M_{a_0(1710)}$ ] and width [ $\Gamma_{a_0(1710)}$ ] of the scalar state  $a_0(1710)$ . The first error is statistical, and the second one is systematic. All values are in units of MeV.

Collaboration	$M_{a_0(1710)}$	$\Gamma_{a_0(1710)}$	Reference
<i>BABAR</i>	$1704 \pm 5 \pm 2$	$110 \pm 15 \pm 11$	[1]
BESIII	$1723 \pm 11 \pm 2$	$140 \pm 14 \pm 4$	[2]
BESIII	$1817 \pm 8 \pm 20$	$97 \pm 22 \pm 15$	[3]

isospin partner  $f_0(1710)$  from various perspectives [4–16]. In Refs. [17, 18], the  $f_0(1710)$ , as a well-established state according to the Review of Particle Physics (RPP) [19], could be dynamically generated from the vector-vector interactions, and one isovector scalar state  $a_0$  with a mass around 1770 MeV was also predicted, the picture of which remains essentially the same when the pseudoscalar-pseudoscalar coupled-channels were taken into account [20]. Based on the SU(6) spin-flavor symmetry, the  $f_0(1710)$  is mostly a  $K^* \bar{K}^*$  bound state, and a  $a_0$  state with a pole position of  $\sqrt{s_R} = (1760, -12)$  was predicted to couple strongly to  $K^* \bar{K}^*$  and  $\phi\rho$  in Ref. [10]. In addition, a scalar state  $a_0$  with a mass of 1744 MeV is also predicted in the approach of the Regge trajectories [21]. In Ref. [12], it was suggested that the  $f_0(1710)$  wave function contains a large  $s\bar{s}$  component, while in Refs. [13–16], the  $f_0(1710)$  was regarded as the candidate of a scalar glueball. Recently, it was shown that the  $a_0(1710)$  as a  $K^* \bar{K}^*$  molecule plays an important role in the three-body interactions of  $\eta K^* \bar{K}^*$ , which could dynamically generate the  $\pi(2070)$  [22].

As shown in Table I, there is not yet a consensus on the

\*Electronic address: wangen@zzu.edu.cn

†Electronic address: lidm@zzu.edu.cn

‡Electronic address: lisheng.geng@buaa.edu.cn

§Electronic address: xiejujun@impcas.ac.cn

mass of the  $a_0(1710)$  experimentally, which could complicate the understanding of its nature. For instance,  $a_0(1710)$  [or  $a_0(1817)$ ] and  $X(1812)$  have been explained as the  $3^3P_0 q\bar{q}$  state by assuming  $a_0(980)$  and  $f_0(980)$  as  $1^3P_0 q\bar{q}$  states [23]. However,  $X(1812)$  was observed in the process  $J/\psi \rightarrow \gamma\phi\omega$  by the BESIII Collaboration [24, 25], and the enhancement near the  $\phi\omega$  threshold, associated to  $X(1812)$ , could be described by the reflection of  $f_0(1710)$ , as discussed in Ref. [8]. Regarding the  $a_0(1710)$  as a  $K^*\bar{K}^*$  molecular state, Refs. [26–30] have successfully described the invariant mass distributions of the processes  $D_s^+ \rightarrow K_S^0 K_S^0 \pi^+$  and  $D_s^+ \rightarrow K_S^0 K^+ \pi^0$  measured by the BESIII Collaboration [2, 3].

Since the peak positions of the  $a_0(1710)$  in the  $K\bar{K}$  invariant mass distributions of the processes  $D_s^+ \rightarrow K_S^0 K_S^0 \pi^+$ ,  $K_S^0 K^+ \pi^0$  observed by the BESIII Collaboration are very close to the boundary region of the  $K\bar{K}$  invariant mass, we have suggested to measure its properties in the process  $\eta_c \rightarrow \bar{K}^0 K^+ \pi^-$  in Ref. [31], and predicted a dip structure around 1.8 GeV, associated with the  $a_0(1710)$ , in the  $\bar{K}^0 K^+$  invariant mass distribution [31], which is consistent with the *BABAR* measurements [32]. In addition, the photo-production process is also proposed to search for the  $a_0(1710)$  in Ref. [33].

The BESIII Collaboration has accumulated  $(10.09 \pm 0.04) \times 10^9$   $J/\psi$  events at the BEPCII collider [34], and the super tau charm facility (STCF) project under development in China is expected to accumulate  $3.4 \times 10^{12}$   $J/\psi$  events per year [35]. Since the dominant decay mode of the  $a_0(1710)$  state is  $K\bar{K}$  within the molecular picture [17, 20], it is natural to search for the scalar  $a_0(1710)$  in the process  $J/\psi \rightarrow a_0(1710)^+ \rho^- \rightarrow \bar{K}^0 K^+ \rho^-$ . It should be stressed that this process has been measured by the *BABAR* Collaboration, and the branching fraction is  $\mathcal{B}(J/\psi \rightarrow K_S^0 K^\pm \rho^\mp) = (1.87 \pm 0.18 \pm 0.34) \times 10^{-3}$  [36]. However, the  $K_S^0 K^\pm$  mass spectrum was not reported by the *BABAR* Collaboration [36].

In this work, we investigate the process  $J/\psi \rightarrow a_0(1710)^+ \rho^- \rightarrow \bar{K}^0 K^+ \rho^-$ , by regarding the  $a_0(1710)$  as a dynamically generated state from the vector-vector interactions in coupled channels. On the other hand, the interactions of vector meson-pseudoscalar meson within the unitary approach could dynamically generate the resonance  $K_1(1270)$  with a two-pole structure [37–39], where the lower pole mainly couples to the  $K^* \pi$  channel, and the higher one couples strongly to the  $K\rho$  channel. Thus, we also take into account the contribution from the intermediate resonance  $K_1(1270)$  in this work, and precise measurements of the process  $J/\psi \rightarrow \bar{K}^0 K^+ \rho^-$  could also shed light on the two-pole structure of  $K_1(1270)$ , which is crucial for us to understand the hadron-hadron interactions [40, 41].

The paper is organized as follows. In Sec. II, we present the theoretical formalism for studying the  $J/\psi \rightarrow \bar{K}^0 K^+ \rho^-$  decay, and in Sec. III, we show our numerical results and discussions, followed by a summary in the last section.

## II. FORMALISM

First, we present the theoretical formalism for studying the process  $J/\psi \rightarrow \bar{K}^0 K^+ \rho^-$  via the  $K^* \bar{K}^*$ ,  $\omega\rho$ , and  $\phi\rho$  final state interactions in coupled channels, which dynamically generate the scalar resonance  $a_0(1710)$  in Subsect. II A. Next, we show the formalism for the process  $J/\psi \rightarrow K_1(1270)^- K^+ [K_1(1270)^0 \bar{K}^0]$  with  $K_1(1270)^- \rightarrow \bar{K}^0 \rho^-$  [ $K_1(1270)^0 \rightarrow K^+ \rho^-$ ] in Subsect. II B. At last, the formalism of the double differential widths for this process is given in Subsect. II C.

### A. Mechanism for the intermediate $a_0(1710)$

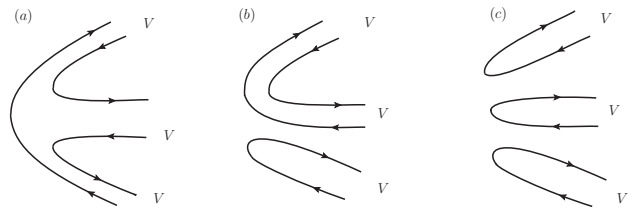


FIG. 1: Diagrammatic expression of  $\langle VVV \rangle$ ,  $\langle VV \rangle \langle V \rangle$ ,  $\langle V \rangle \langle V \rangle \langle V \rangle$  terms in Eq. (1).

As done in Refs. [26, 27, 31], the scalar meson  $a_0(1710)$  is regarded as a vector-vector molecular state [17, 18]. To study the role of  $a_0(1710)$  in the  $J/\psi \rightarrow \rho^- K^+ \bar{K}^0$  decay, one needs to firstly produce the meson  $\rho^-$  and a vector-vector pair, then the final state interactions of the vector-vector pair will produce the  $a_0(1710)$ , which decays into  $K^+ \bar{K}^0$  in the final state. Considering that the  $J/\psi$  is a flavor singlet, we could introduce the combination modes in the primary vertex [42–44], whose diagrammatic expression is depicted in Fig. 1,

$$\langle VVV \rangle, \quad \langle VV \rangle \langle V \rangle, \quad \langle V \rangle \langle V \rangle \langle V \rangle, \quad (1)$$

where  $V$  is the matrix of the SU(3) vector mesons [42–47],

$$V = \begin{pmatrix} \frac{\rho^0}{\sqrt{2}} + \frac{\omega}{\sqrt{2}} & \rho^+ & K^{*+} \\ \rho^- & -\frac{\rho^0}{\sqrt{2}} + \frac{\omega}{\sqrt{2}} & K^{*0} \\ K^{*-} & \bar{K}^{*0} & \phi \end{pmatrix}, \quad (2)$$

with the symbol ' $\langle \dots \rangle$ ' stands for the trace of the SU(3) matrices. Since no term contains  $\rho^-$  in  $\langle V \rangle \langle V \rangle \langle V \rangle$ , we do not take this combination in our work. One could obtain the relevant contributions by isolating the terms containing  $\rho^-$ , as follows,

$$\langle VVV \rangle : \alpha \times \left[ \frac{\rho^+ \rho^0}{\sqrt{2}} + 3\sqrt{2}\omega\rho^+ + 3\bar{K}^{*0} K^{*+} \right] \rho^- \quad (3)$$

$$\langle VV \rangle \langle V \rangle : \beta \times \left[ 2\sqrt{2}\omega\rho^+ + 2\phi\rho^+ \right] \rho^-. \quad (4)$$

Here, two parameters  $\alpha$  and  $\beta$  are introduced to account for the weights of  $\langle VVV \rangle$  and  $\langle VV \rangle \langle V \rangle$  structures,

respectively. It is concluded in Refs. [17, 48, 49] that the  $\langle VVV \rangle$  one was favored and the best ratio  $\beta/\alpha = 0.32$  was obtained by fitting to the experimental measurements of the process  $J/\psi \rightarrow \phi VV$  [17, 49], thus we will use this finding and take  $\alpha = 1$  and  $\beta = 0.32$  in this work.

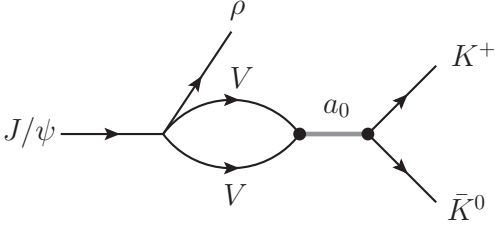


FIG. 2: Diagram for the process  $J/\psi \rightarrow VV\rho^- \rightarrow a_0(1710)^+\rho^- \rightarrow K^+\bar{K}^0\rho^-$  with  $VV$  stands for  $\bar{K}^{*0}K^{*+}$ ,  $\omega\rho^+$  and  $\phi\rho^+$ .

In the molecular picture, the  $a_0(1710)$  is dynamically generated from the  $S$ -wave  $K^*\bar{K}^*$ ,  $\omega\rho$ , and  $\phi\rho$  interactions in coupled channels [17, 18]<sup>1</sup>, and then decays into the final state  $\bar{K}^0K^+$ , as depicted in Fig. 2. The decay amplitude of Fig. 2 can be written as,

$$\begin{aligned} \mathcal{M}_a = & V_p \times [3\alpha G_{\bar{K}^{*0}K^{*+}} t_{\bar{K}^{*0}K^{*+} \rightarrow \bar{K}^0K^+} \\ & + (2\sqrt{2}\beta + 3\sqrt{2}\alpha) G_{\omega\rho^+} t_{\omega\rho^+ \rightarrow \bar{K}^0K^+} \\ & + 2\beta\phi\rho^+ G_{\phi\rho^+} t_{\phi\rho^+ \rightarrow \bar{K}^0K^+}], \end{aligned} \quad (5)$$

where  $V_p$  is a global factor, and  $t_{\bar{K}^{*0}K^{*+} \rightarrow \bar{K}^0K^+}$ ,  $t_{\omega\rho^+ \rightarrow \bar{K}^0K^+}$ , and  $t_{\phi\rho^+ \rightarrow \bar{K}^0K^+}$  are the transition amplitudes.  $G_{\bar{K}^{*0}K^{*+}}$ ,  $G_{\omega\rho^+}$ , and  $G_{\phi\rho^+}$  are the loop functions for the  $\bar{K}^{*0}K^{*+}$ ,  $\omega\rho^+$ , and  $\phi\rho^+$  channels, respectively, and read [17, 50],

$$\begin{aligned} G_i(M_{\bar{K}^0K^+}) = & \int_{m_{1-}^2}^{m_{1+}^2} \int_{m_{2-}^2}^{m_{2+}^2} d\tilde{m}_1^2 d\tilde{m}_2^2 \times \\ & \omega(\tilde{m}_1^2) \omega(\tilde{m}_2^2) \tilde{G}(M_{\bar{K}^0K^+}, \tilde{m}_1^2, \tilde{m}_2^2), \end{aligned} \quad (6)$$

where

$$\omega(\tilde{m}_i^2) = \frac{1}{N} \left( -\frac{1}{\pi} \right) \text{Im} \left[ \frac{1}{\tilde{m}_i^2 - m_{V_i}^2 + i\Gamma(\tilde{m}_i^2)\tilde{m}_i} \right], \quad (7)$$

$$N = \int_{\tilde{m}_{i-}^2}^{\tilde{m}_{i+}^2} d\tilde{m}_i^2 \left( -\frac{1}{\pi} \right) \text{Im} \left[ \frac{1}{\tilde{m}_i^2 - m_{V_i}^2 + i\Gamma(\tilde{m}_i^2)\tilde{m}_i} \right], \quad (8)$$

$$\Gamma(\tilde{m}_i^2) = \Gamma_{V_i} \frac{\tilde{k}^3}{k^3} \Theta(\tilde{m} - m_{P_1} - m_{P_2}), \quad (9)$$

$$\tilde{k} = \frac{\lambda^{\frac{1}{2}}(\tilde{m}_i^2, m_{P_1}^2, m_{P_2}^2)}{2\tilde{m}_i}, \quad k = \frac{\lambda^{\frac{1}{2}}(m_{V_i}^2, m_{P_1}^2, m_{P_2}^2)}{2m_{V_i}}, \quad (10)$$

with the Källén function  $\lambda(x, y, z) = x^2 + y^2 + z^2 - 2xy - 2xz - 2yz$ . Here, we consider the decay channels  $\pi\pi$  and  $K\pi$  for the vector mesons  $\rho$  and  $K^*$ , respectively, and neglect the small widths of  $\omega$  ( $\Gamma_\omega = 8.68$  MeV) and  $\phi$  ( $\Gamma_\phi = 4.249$  MeV). Taking the vector  $K^*$  for example,  $m_{1+}^2 = (m_{K^*} + 2\Gamma_{K^*})^2$  and  $m_{1-}^2 = (m_{K^*} - 2\Gamma_{K^*})^2$ . Similarly, one can obtain  $m_{1+}^2$  and  $m_{1-}^2$  for the  $\rho$  meson. The masses, widths, and spin-parities of the involved particles are taken from the RPP [19], as listed in Table II.

TABLE II: Masses, widths, and spin-parities of the involved particles in this work. All values are in units of MeV.

state	mass	width	spin-parity ( $J^P$ )
$J/\psi$	3096.900	0.0926	$1^-$
$\rho^{\pm,0}$	775.26	149.1	$1^-$
$\bar{K}^0$	497.611	—	$0^-$
$K^\pm$	493.677	—	$0^-$
$K^*$	893.6	49.1	$1^-$
$\omega$	782.66	8.68	$1^-$
$\phi$	1019.461	4.249	$1^-$
$K_1(1270)$	1284	146	$1^+$

The loop function  $\tilde{G}$  in Eq. (6) is for stable particles, and in the dimensional regularization scheme, it can be written as [51],

$$\begin{aligned} \tilde{G} = & \frac{1}{16\pi^2} \left\{ a_\mu + \text{In} \frac{m_1^2}{\mu^2} + \frac{m_2^2 - m_1^2 + s}{2s} \text{In} \frac{m_2^2}{m_1^2} \right. \\ & \frac{p}{\sqrt{s}} \left[ \text{In}(s - (m_2^2 - m_1^2) + 2p\sqrt{s}) \right. \\ & + \text{In}(s + (m_2^2 - m_1^2) + 2p\sqrt{s}) \\ & - \text{In}(-s + (m_2^2 - m_1^2) + 2p\sqrt{s}) \\ & \left. \left. - \text{In}(-s - (m_2^2 - m_1^2) + 2p\sqrt{s}) \right] \right\}, \end{aligned} \quad (11)$$

with

$$p = \frac{\lambda^{1/2}(s, m_1^2, m_2^2)}{2\sqrt{s}}, \quad (12)$$

where  $a_\mu$  is the subtraction constant,  $\mu$  is the dimensional regularization scale, and  $s = M_{\bar{K}^0K^+}^2$ . In this work, we take  $a_\mu = -1.726$  and  $\mu = 1000$  MeV as used in Ref. [17]. It is worth mentioning that any change in  $\mu$  could be reabsorbed by a change in  $a_\mu$  through  $a_{\mu'} - a_\mu = \ln(\mu'^2/\mu^2)$ , which implies that the loop function  $\tilde{G}$  is scale independent [52].

To show the influence of the widths of vector mesons on the loop functions, we have calculated the loop functions  $G_{\phi\rho^+}$  and  $\tilde{G}_{\phi\rho^+}$  as functions of the  $\bar{K}^0K^+$  invariant mass<sup>2</sup>, as presented in Fig. 3. The blue long-dashed

<sup>1</sup> It should be noted that, the conservation of  $G$ -parity forbids the coupling of  $a_0(1710)$  to the channel  $\rho\rho$ .

<sup>2</sup> One can find the invariant mass distributions of the loop func-

and red dot-dashed curves correspond to the real and imaginary parts of the loop function  $G$ , considering the width of  $\rho$ . In contrast, the green solid and purple dotted curves correspond to the real and imaginary parts of the loop function  $\tilde{G}$  without the contribution from the  $\rho$  width, respectively. One can find that the loop functions  $G$ , considering the width of the vector meson, become smoother around the threshold of the  $\phi\rho$ .

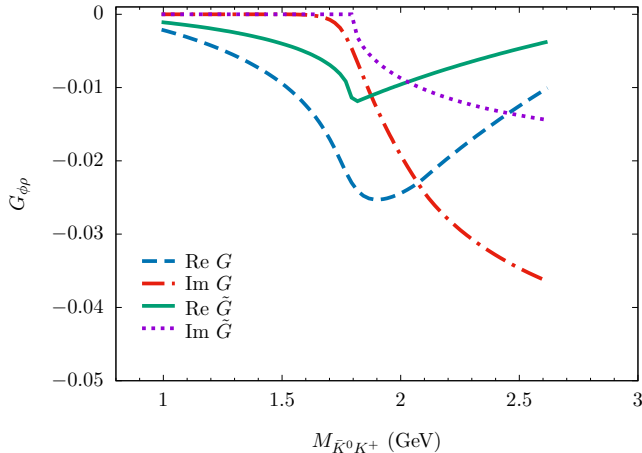


FIG. 3: Real and imaginary parts of the loop functions  $G_{\phi\rho}$  and  $\tilde{G}_{\phi\rho}$  as a function of the  $\bar{K}^0 K^+$  invariant mass. The blue long-dashed and red dot-dashed curves correspond to the real and imaginary parts of the loop function  $G$ , considering the width of  $\rho$ . Meanwhile, the green solid and purple dotted curves correspond to the real and imaginary parts of the loop function  $\tilde{G}$  without the contribution from the  $\rho$  width, respectively.

TABLE III: Mass, width, and coupling constants of the scalar  $a_0(1710)$  [17]. All values are in units of MeV.

parameters	value
mass	1777
width	148
$\Gamma_{K\bar{K}}$	36
$g_{K\bar{K}}$	1966
$g_{\rho\rho}$	0
$g_{K^*\bar{K}^*}$	(7525, -i1529)
$g_{\omega\rho}$	(-4042, i1391)
$g_{\phi\rho}$	(4998, -i1872)
$g_{K\rho}$	(4804, i395)

On the other hand, the transition amplitudes  $t_{i\rightarrow\bar{K}^0 K^+}$

tions  $\tilde{G}_{\bar{K}^*0 K^{*+}}$  and  $\tilde{G}_{\omega\rho}$  in Refs. [26, 31].

in Eq. (5) can be written as,

$$t_{i\rightarrow\bar{K}^0 K^+} = \frac{g_i \times g_{K\bar{K}}}{M_{\bar{K}^0 K^+}^2 - M_{a_0}^2 + iM_{a_0}\Gamma_{a_0}}, \quad (13)$$

where  $M_{a_0}$  and  $\Gamma_{a_0}$  are the mass and width of the  $a_0(1710)$ , respectively, and we take their values from Refs. [17, 53], which are tabulated in Table III.  $g_i$  are the coupling constants of  $a_0(1710)$  to  $K^*\bar{K}^*$ ,  $\omega\rho$ , and  $\phi\rho^+$ , whose values are determined in Ref. [17], while the coupling  $g_{K\bar{K}}$  is determined from the partial decay width of  $a_0(1710) \rightarrow K\bar{K}$ ,

$$\Gamma_{K\bar{K}} = \frac{g_{K\bar{K}}^2 |\vec{p}_K|}{8\pi M_{a_0}^2}, \quad (14)$$

where  $\vec{p}_K$  is the three-momentum of the  $K$  or  $\bar{K}$  meson in the  $a_0(1710)$  rest frame,

$$|\vec{p}_K| = \frac{\lambda^{1/2}(M_{a_0}^2, m_{\bar{K}}^2, m_K^2)}{2M_{a_0}}. \quad (15)$$

With the partial decay width  $\Gamma_{K\bar{K}} = 36$  MeV predicted by Ref. [17], one can only obtain the absolute value of the coupling constant, but not the phase, thus by assuming that  $g_{K\bar{K}}$  is real and positive we take  $g_{K\bar{K}} = 1966$  MeV, as done in Refs. [26, 27].

## B. Mechanism for the intermediate $K_1(1270)$

In Fig. 4, we show the Dalitz plot for the process  $J/\psi \rightarrow \bar{K}^0 K^+ \rho^-$ , and one can find that the contribution from the  $K_1(1270)$  (the green band) could interfere with the one from the  $a_0(1710)$  (the red band) close to the  $K\rho$  threshold. Since the  $K_1(1270)$  state could be dynamically generated from the interaction of vector meson-pseudoscalar meson [37, 38, 38], the  $K^+\rho^-$  and  $\bar{K}^0\rho^-$  could undergo the  $S$ -wave final state interaction, which will generate the  $K_1(1270)$  state, followed by the decay  $K_1(1270) \rightarrow K\rho$ , as depicted in Fig. 5.

TABLE IV: Pole positions and coupling constants of the two poles of the  $K_1(1270)$  [37]. All values are in units of MeV.

	1st pole	2nd pole
pole position $\sqrt{s_0}$	1195 - i123	1284 - i73
$g_{K\rho}$	-1671 + i1599	4804 + i395

The decay amplitude for  $J/\psi \rightarrow \bar{K}^0 K_1(1270)^- \rightarrow \bar{K}^0 K^+ \rho^-$  of Fig. 5(a) can be written as,

$$\mathcal{M}_b = V_p' \times G_{K^+\rho^-} t_{K^+\rho^- \rightarrow K^+\rho^-}, \quad (16)$$

where  $V_p'$  stands for the weight of contribution from the  $K_1(1270)^0$ , and the  $t_{K^+\rho^- \rightarrow K^+\rho^-}$  is the transition amplitude, which can be written as

$$t_{K^+\rho^- \rightarrow K^+\rho^-} = \frac{g_{K^+\rho^-} g_{K^+\rho^-}}{M_{K^+\rho^-}^2 - M_{K_1}^2 + iM_{K_1}\Gamma_{K_1}}, \quad (17)$$

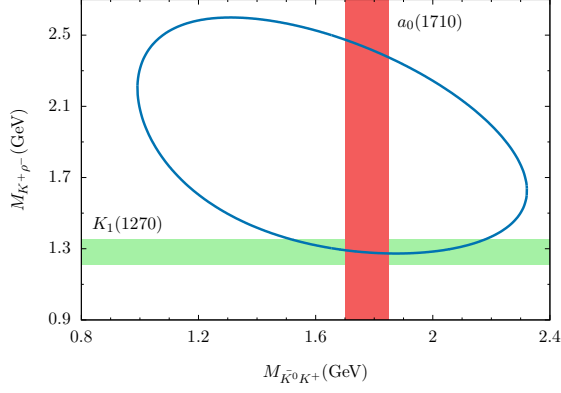


FIG. 4: The Dalitz plot for the  $J/\psi \rightarrow \bar{K}^0 K^+ \rho^-$ . The red band stands for the region of  $M_{a_0} \pm \frac{1}{2}\Gamma_{a_0}$  where the predicted  $a_0(1710)$  state lies. The green band stands for the region of  $M_{K_1} \pm \frac{1}{2}\Gamma_{K_1}$  where the  $K_1(1270)$  state lies.

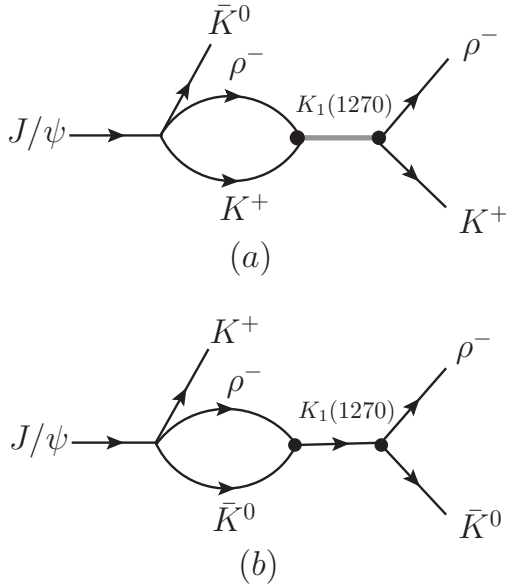


FIG. 5: Diagrams for  $J/\psi \rightarrow \bar{K}^0 K^+ \rho^-$  via the intermediate  $K_1(1270)^0$  (a) and  $K_1(1270)^-$  (b), followed by the decay  $K_1(1270)^{0,-} \rightarrow K^+ \rho^- / \bar{K}^0 \rho^-$ .

where  $M_{K^+ \rho^-}$  is the invariant mass of the  $K^+ \rho^-$  system, and  $g_{K^+ \rho^-}$  denotes the coupling constant. In this work, we adopt the value  $g_{K^+ \rho^-} = (4804 + i395)$  MeV of Table IV, where the axial-vector meson  $K_1(1270)$  is dynamically generated from the pseudoscalar meson-vector meson interactions. Since the higher pole of the  $K_1(1270)$  mainly couples to the  $K\rho$  channel, we can relate the mass and width of the  $K_1(1270)$  with the higher pole position of Table IV, i.e.  $M_{K_1} = \text{Re}\sqrt{s_0}$  and  $\Gamma_{K_1} = 2\text{Im}\sqrt{s_0}$ . Similarly, the amplitude of the process  $J/\psi \rightarrow K^+ K_1(1270)^- \rightarrow K^+ \bar{K}^0 \rho^-$ , as depicted in

Fig. 5(b), can be expressed as,

$$\mathcal{M}_c = V'_p \times G_{\bar{K}^0 \rho^-} t_{\bar{K}^0 \rho^- \rightarrow \bar{K}^0 \rho^-}, \quad (18)$$

$$t_{\bar{K}^0 \rho^- \rightarrow \bar{K}^0 \rho^-} = \frac{g_{\bar{K}^0 \rho^-} g_{\bar{K}^0 \rho^-}}{M_{\bar{K}^0 \rho^-}^2 - M_{K_1}^2 + iM_{K_1} \Gamma_{K_1}}, \quad (19)$$

where  $M_{\bar{K}^0 \rho^-}$  is the  $\bar{K}^0 \rho^-$  invariant mass, and  $g_{\bar{K}^0 \rho^-}$  is the coupling constant,  $g_{\bar{K}^0 \rho^-} = g_{K^+ \rho^-} = (4804 + i395)$  MeV in this work. We take the same weight  $V'_p$  for the contributions from the  $K_1(1270)^0$  and  $K_1(1270)^-$ .

According to Eqs. (6) and (11), we have also calculated the loop function  $G_{K^+ \rho^-} / G_{\bar{K}^0 \rho^-}$  and  $\tilde{G}_{K^+ \rho^-} / \tilde{G}_{\bar{K}^0 \rho^-}$  as functions of the  $K^+ \rho^-$  and  $\bar{K}^0 \rho^-$  invariant masses, respectively, as presented in Figs. 6 and 7. One can find that the loop functions  $G$  become smoother around the threshold when considering the width of the  $\rho$ .

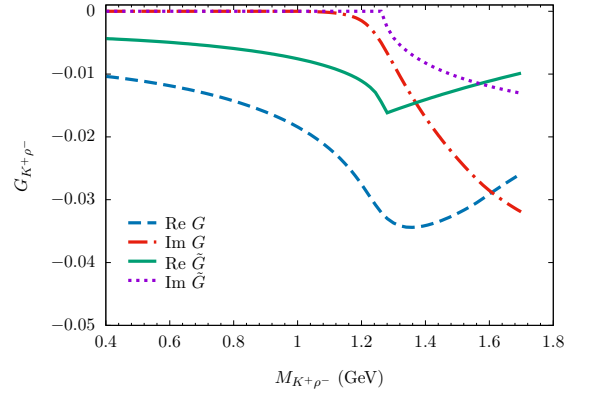


FIG. 6: Real and imaginary parts of the loop functions  $G_{K^+ \rho^-}$  and  $\tilde{G}_{K^+ \rho^-}$  as a function of the  $K^+ \rho^-$  invariant mass. The notations of the curves are the same as those of Fig. 3.

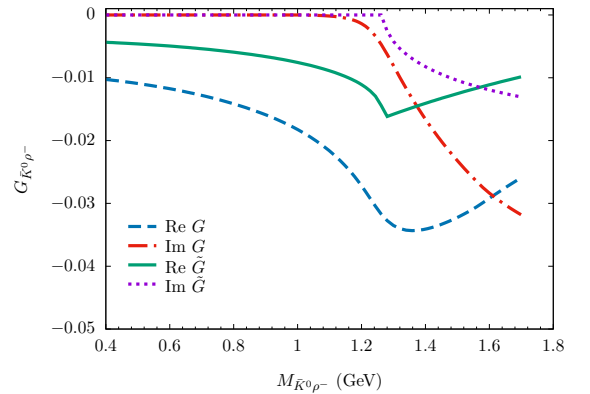


FIG. 7: Real and imaginary parts of the loop functions  $G_{\bar{K}^0 \rho^-}$  and  $\tilde{G}_{\bar{K}^0 \rho^-}$  as a function of the  $\bar{K}^0 \rho^-$  invariant mass. The notations of the curves are the same as those of Fig. 3.



### C. Invariant mass distributions

With the amplitudes obtained above, we can write down the total decay amplitude of  $J/\psi \rightarrow \bar{K}^0 K^+ \rho^-$  as follows,

$$\mathcal{M} = \mathcal{M}_a + \mathcal{M}_b + \mathcal{M}_c, \quad (20)$$

and the double differential widths of the process  $J/\psi \rightarrow \bar{K}^0 K^+ \rho^-$  are

$$\frac{d^2\Gamma}{dM_{\bar{K}^0 K^+} dM_{K^+ \rho^-}} = \frac{M_{\bar{K}^0 K^+} M_{K^+ \rho^-}}{128\pi^3 m_{J/\psi}^3} |\mathcal{M}|^2, \quad (21)$$

$$\frac{d^2\Gamma}{dM_{\bar{K}^0 K^+} dM_{\bar{K}^0 \rho^-}} = \frac{M_{\bar{K}^0 K^+} M_{\bar{K}^0 \rho^-}}{128\pi^3 m_{J/\psi}^3} |\mathcal{M}|^2. \quad (22)$$

Furthermore, one can easily obtain  $d\Gamma/dM_{\bar{K}^0 K^+}$ ,  $d\Gamma/dM_{\bar{K}^0 \rho^-}$ , and  $d\Gamma/dM_{K^+ \rho^-}$  by integrating over each of the invariant mass variables with the limits of the Dalitz plot given in the RPP [19]. However, since the final meson  $\rho^-$  has a large width ( $\sim 149.1$  MeV), and the  $K_1(1270)$  mass is very close to the  $K\rho$  threshold (as shown by Fig. 4), one needs to take into account its finite width by folding with the vector-meson  $\rho^-$  spectral function for the invariant mass distributions [39], as follows,

$$\frac{d\tilde{\Gamma}}{dM_{12}} = \int_{m_{\rho^-} - 2\Gamma_{\rho^-}}^{m_{\rho^-} + 2\Gamma_{\rho^-}} d\hat{m}_{\rho^-} \left[ \frac{d\Gamma}{dM_{12}} \times \omega(\hat{m}_{\rho^-}^2) \right], \quad (23)$$

where the mass  $m_{\rho^-}$  in  $d\Gamma/dM_{12}$  should be replaced by  $\hat{m}_{\rho^-}$ . For example, the differential width  $d\tilde{\Gamma}/dM_{\bar{K}^0 K^+}$  of the process  $J/\psi \rightarrow \bar{K}^0 K^+ \rho^-$  becomes,

$$\begin{aligned} \frac{d\tilde{\Gamma}}{dM_{\bar{K}^0 K^+}} &= \int_{m_{\rho^-} - 2\Gamma_{\rho^-}}^{\min(m_{\rho^-} + 2\Gamma_{\rho^-}, m_{J/\psi} - M_{\bar{K}^0 K^+})} d\hat{m}_{\rho^-} \\ &\times \int_{M_{K^+ \rho^-}^{\min}}^{M_{K^+ \rho^-}^{\max}} dM_{K^+ \rho^-} \\ &\times \frac{M_{\bar{K}^0 K^+} M_{K^+ \rho^-}}{128\pi^3 m_{J/\psi}^3} |\mathcal{M}|^2 \times \omega(\hat{m}_{\rho^-}^2), \quad (24) \end{aligned}$$

where the range of  $M_{\bar{K}^0 K^+}$  is,

$$m_{\bar{K}^0} + m_{K^+} < M_{\bar{K}^0 K^+} < m_{J/\psi} - m_{\rho^-} + 2\Gamma_{\rho^-}, \quad (25)$$

and the upper and lower limits for  $M_{K^+ \rho^-}$  are,

$$\begin{aligned} \left( M_{K^+ \rho^-}^{\max} \right)^2 &= \left( E_{K^+}^* + E_{\rho^-}^* \right)^2 - \\ &\quad \left( \sqrt{E_{K^+}^{*2} - m_{K^+}^2} - \sqrt{E_{\rho^-}^{*2} - \hat{m}_{\rho^-}^2} \right)^2 \\ \left( M_{K^+ \rho^-}^{\min} \right)^2 &= \left( E_{K^+}^* + E_{\rho^-}^* \right)^2 - \\ &\quad \left( \sqrt{E_{K^+}^{*2} - m_{K^+}^2} + \sqrt{E_{\rho^-}^{*2} - \hat{m}_{\rho^-}^2} \right)^2, \end{aligned}$$

where  $E_{K^+}^*$  and  $E_{\rho^-}^*$  are the energies of  $K^+$  and  $\rho^-$  in the  $\bar{K}^0 \rho^-$  rest frame, respectively,

$$\begin{aligned} E_{K^+}^* &= \frac{M_{\bar{K}^0 K^+}^2 - m_{\bar{K}^0}^2 + m_{K^+}^2}{2M_{\bar{K}^0 K^+}}, \\ E_{\rho^-}^* &= \frac{m_{J/\psi}^2 - M_{\bar{K}^0 K^+}^2 - \hat{m}_{\rho^-}^2}{2M_{\bar{K}^0 K^+}}. \quad (26) \end{aligned}$$

### III. RESULTS AND DISCUSSION

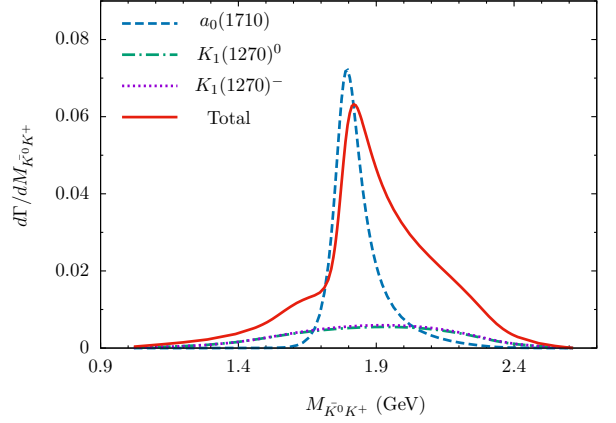


FIG. 8:  $\bar{K}^0 K^+$  invariant mass distribution of the process  $J/\psi \rightarrow \bar{K}^0 K^+ \rho^-$ . The results are obtained with Eq. (23), where the width of final  $\rho^-$  is considered. The red-solid curve stands for the total contribution, while the blue-dashed curve, the green-dot-dashed curve, and purple-dotted curve correspond to the contributions from the  $a_0(1710)$  state, the intermediate  $K_1(1270)^0$ , and  $K_1(1270)^-$ , respectively.

In our formalism, there are two unknown parameters,  $V_p$  for the weight of the  $a_0(1710)$  contribution and  $V_p'$  for the one of the intermediate  $K_1(1270)$  contribution. Since there are some similarities between the processes  $J/\psi \rightarrow VVV$  and  $J/\psi \rightarrow VPP$ , it is expected that  $V_p$  and  $V_p'$  are of the same order of magnitude. Thus, we first take  $V_p = V_p'$  and discuss the influence on our results of different values of  $V_p$  and  $V_p'$ .

In Fig. 8, we show the  $\bar{K}^0 K^+$  invariant mass distribution of the process  $J/\psi \rightarrow \bar{K}^0 K^+ \rho^-$ . The red-solid curve stands for the total contributions from the  $a_0(1710)$  state and the axial-vector  $K_1(1270)$  meson, while the blue-dashed curve corresponds to the contribution from the  $a_0(1710)$  state. Moreover, the green-dot-dashed and purple-dotted curves correspond to the contributions from the intermediate  $K_1(1270)^0$  and  $K_1(1270)^-$ , respectively. One can find a clear peak structure around 1.8 GeV, which could be associated with the scalar  $a_0(1710)$ . The intermediate resonances  $K_1(1270)^0$  and  $K_1(1270)^-$  give the smooth contributions in the region of 1.4  $\sim$  2.4 GeV, which is due to that the  $K_1(1270)$  couples to  $K\rho$  in  $S$ -wave.

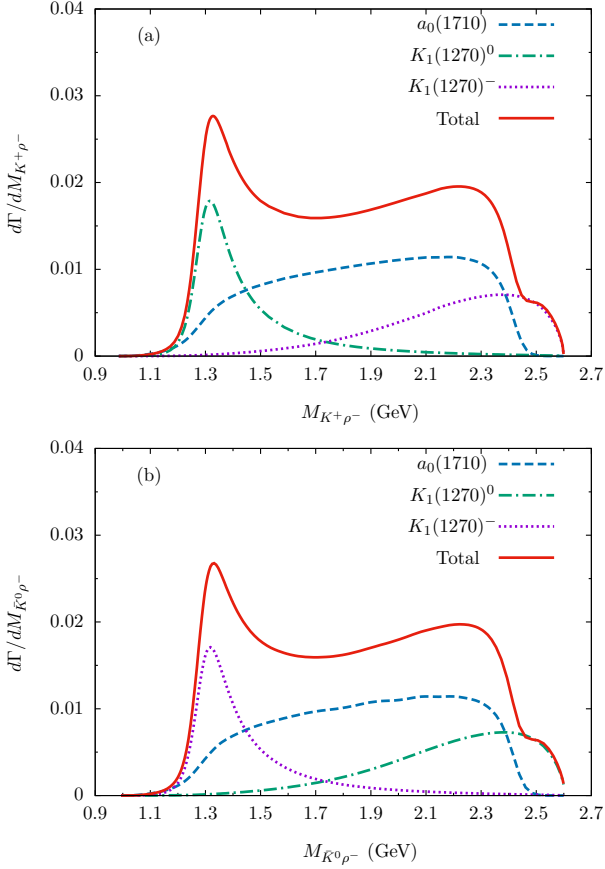


FIG. 9:  $K^+\rho^-$  (a) and  $\bar{K}^0\rho^-$  (b) invariant mass distributions of the process  $J/\psi \rightarrow \bar{K}^0 K^+ \rho^-$ . The explanations of the curves are the same as those of Fig. 8.

Next, we have predicted the  $K^+\rho^-$  and  $\bar{K}^0\rho^-$  invariant mass distributions of the process  $J/\psi \rightarrow \bar{K}^0 K^+ \rho^-$  in Figs. 9(a) and 9(b), respectively. One can see the clear peaks of the  $K_1(1270)^0$  and  $K_1(1270)^-$  around 1.3 GeV. It should be stressed that the axial vector  $K_1(1270)$  is predicted to have a two-pole structure, the lower pole is around 1200 MeV, coupled strongly to the  $K^*\pi$  channel, which the higher pole is around 1280 MeV, coupled strongly to the  $K\rho$  channels [37].

As we discussed above, since the higher pole of  $K_1(1270)$  mainly couples to the  $K\rho$  channel, we have adopted the pole position and coupling constant of the higher pole in Eq. (19). To show the difference between the two poles of the  $K_1(1270)$ , we have calculated the  $\bar{K}^0 K^+$ ,  $K^+\rho^-$ , and  $\bar{K}^0\rho^-$  invariant mass distributions for the process  $J/\psi \rightarrow \bar{K}^0 K^+ \rho^-$  with the pole position and coupling constant of the lower pole of Table IV in Eq. (19), as shown in Fig. 10. Because the coupling of the lower pole to  $K\rho$  is smaller and the width is larger, the contribution from the lower pole of the  $K_1(1270)$  is very small. For the contributions from the lower pole and the higher pole to have the same order of magnitude, we take  $V'_p/V_p = 8.0$  in the results of Fig. 10. In the  $\bar{K}^0 K^+$  invariant mass distribution of Fig. 10(a), one

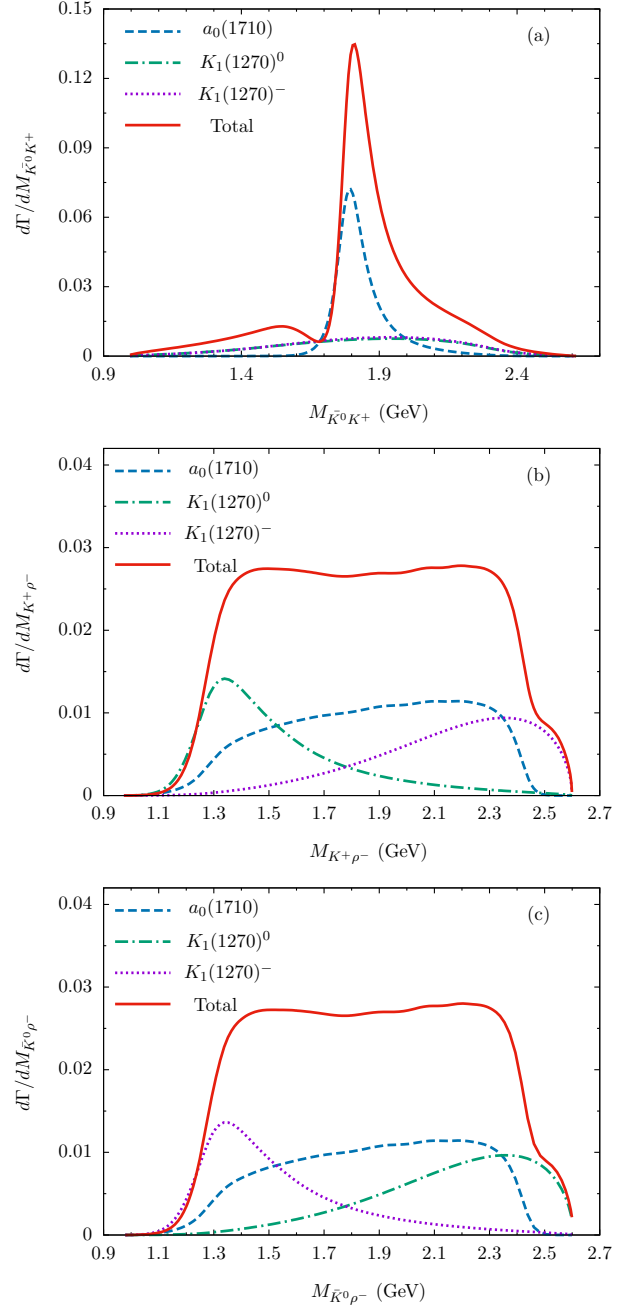


FIG. 10: The  $\bar{K}^0 K^+$  (a),  $K^+\rho^-$  (b) and  $\bar{K}^0\rho^-$  (c) invariant mass distributions of the process  $J/\psi \rightarrow \bar{K}^0 K^+ \rho^-$  with the parameters of lower pole of  $K_1(1270)$ . The explanations of the curves are the same as those of Fig. 8.

can find the clear peak structure around 1.8 GeV. However, in the  $\bar{K}^0\rho^-$  and  $K^+\rho^-$  invariant mass distributions of Figs. 10(b) and 10(c), only an enhancement structure appears. Thus, future measurements of  $\bar{K}^0\rho^-$  and  $K^+\rho^-$  invariant mass distributions could shed light on the two-pole structure of the  $K_1(1270)$ .

In addition, we take different ratios of  $V'_p/V_p = 0.5, 1.0, 1.5$ , and show the  $\bar{K}^0 K^+$ ,  $K^+\rho^-$ , and  $\bar{K}^0\rho^-$

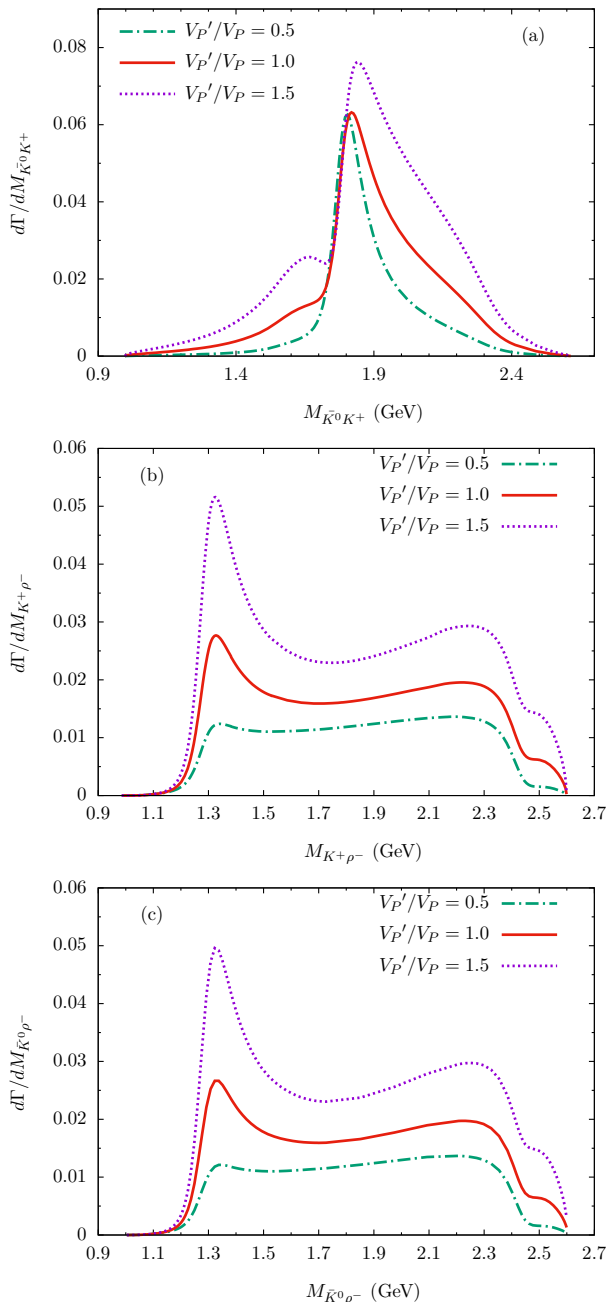


FIG. 11:  $\bar{K}^0 K^+$ ,  $K^+ \rho^-$ , and  $\bar{K}^0 \rho^-$  invariant mass distributions of the process  $J/\psi \rightarrow \bar{K}^0 K^+ \rho^-$  with  $V_p'/V_p = 0.5, 1.0, 1.5$ .

invariant mass distributions for the process  $J/\psi \rightarrow \bar{K}^0 K^+ \rho^-$  in Figs. 11(a), 11(b), and 11(c), respectively.

One can find that the peak structure of the  $a_0(1710)$  in the  $\bar{K}^0 K^+$  invariant mass distribution remains similar for different values of  $V_p'/V_p$ , and the peak structures of the  $K_1(1270)$  become clearer for larger values of  $V_p'/V_p$ .

#### IV. SUMMARY

Assuming the  $a_0(1710)$  as a  $K^* \bar{K}^*$  molecular state, we have investigated the process  $J/\psi \rightarrow \bar{K}^0 K^+ \rho^-$  by taking into account the contribution from the  $S$ -wave  $\omega \rho^+$ ,  $\bar{K}^{*0} K^{*+}$ , and  $\phi \rho$  interactions, as well as the contribution from the intermediate resonance  $K_1(1270)$ .

We have predicted one peak structure around 1.8 GeV in the  $\bar{K}^0 K^+$  invariant mass distribution, which could be associated with the scalar meson  $a_0(1710)$ . Furthermore, we have also predicted the  $K^+ \rho^-$  and  $\bar{K}^0 \rho^-$  invariant mass distributions of the process  $J/\psi \rightarrow \bar{K}^0 K^+ \rho^-$ , and find clear peaks of the resonance  $K_1(1270)^{0,-}$ . Considering the two-pole structure of the  $K_1(1270)$ , we have also calculated the results adopting parameters of the lower pole and find an enhancement structure near 1.3 GeV in the  $K^+ \rho^-$  and  $\bar{K}^0 \rho^-$  invariant mass distributions, which implies that future measurements of the  $K^+ \rho^-$  and  $\bar{K}^0 \rho^-$  invariant mass distributions could shed light on the two-pole structure of the  $K_1(1270)$ .

Finally, considering different weights ratio  $V_p'/V_p = 0.5, 1.0, 1.5$  of contributions from  $a_0(1710)$  and  $K_1(1270)$ , we have shown the  $\bar{K}^0 K^+$ ,  $K^+ \rho^-$  and  $\bar{K}^0 \rho^-$  invariant mass distributions of the process  $J/\psi \rightarrow \bar{K}^0 K^+ \rho^-$ , and find that the peak structure of  $a_0(1710)$  remains essentially the same. We hope that our theoretical predictions could be tested by the BESIII and BelleII experiments and the planned STCF in the future, and precise measurements of the process  $J/\psi \rightarrow \bar{K}^0 K^+ \rho^-$  could shed light on the nature of the scalar  $a_0(1710)$  and the axial-vector  $K_1(1270)$ .

#### Acknowledgments

This work is supported by the Natural Science Foundation of Henan under Grant No. 222300420554 and No. 232300421140. This work is partly supported by the National Natural Science Foundation of China under Grants Nos. 12075288, 11975041, 11961141004, 12361141819, and 12192263, the Project of Youth Backbone Teachers of Colleges and Universities of Henan Province (2020GGJS017), and the Open Project of Guangxi Key Laboratory of Nuclear Physics and Nuclear Technology, No. NLK2021-08. It is also partly supported by the Youth Innovation Promotion Association CAS.

- [1] J. P. Lees *et al.* [BaBar], Phys. Rev. D **104** (2021) no.7, 072002 doi:10.1103/PhysRevD.104.072002 [arXiv:2106.05157 [hep-ex]].  
 [2] M. Ablikim *et al.* [BESIII], Phys. Rev. D **105** (2022)

- no.5, L051103 doi:10.1103/PhysRevD.105.L051103 [arXiv:2110.07650 [hep-ex]].  
 [3] M. Ablikim *et al.* [BESIII], Phys. Rev. Lett. **129** (2022) no.18, 18 doi:10.1103/PhysRevLett.129.182001



- [arXiv:2204.09614 [hep-ex]].
- [4] H. Nagahiro, L. Roca, E. Oset and B. S. Zou, Phys. Rev. D **78** (2008), 014012 doi:10.1103/PhysRevD.78.014012 [arXiv:0803.4460 [hep-ph]].
- [5] T. Branz, L. S. Geng and E. Oset, Phys. Rev. D **81** (2010), 054037 doi:10.1103/PhysRevD.81.054037 [arXiv:0911.0206 [hep-ph]].
- [6] L. S. Geng, F. K. Guo, C. Hanhart, R. Molina, E. Oset and B. S. Zou, Eur. Phys. J. A **44** (2010), 305-311 doi:10.1140/epja/i2010-10971-5 [arXiv:0910.5192 [hep-ph]].
- [7] J. J. Xie and E. Oset, Phys. Rev. D **90** (2014) no.9, 094006 doi:10.1103/PhysRevD.90.094006 [arXiv:1409.1341 [hep-ph]].
- [8] A. Martinez Torres, K. P. Khemchandani, F. S. Navarra, M. Nielsen and E. Oset, Phys. Lett. B **719** (2013), 388-393 doi:10.1016/j.physletb.2013.01.036 [arXiv:1210.6392 [hep-ph]].
- [9] Z. L. Wang and B. S. Zou, Phys. Rev. D **104** (2021) no.11, 114001 doi:10.1103/PhysRevD.104.114001 [arXiv:2107.14470 [hep-ph]].
- [10] C. Garcia-Recio, L. S. Geng, J. Nieves and L. L. Salcedo, Phys. Rev. D **83** (2011), 016007 doi:10.1103/PhysRevD.83.016007 [arXiv:1005.0956 [hep-ph]].
- [11] C. Garcia-Recio, L. S. Geng, J. Nieves, L. L. Salcedo, E. Wang and J. J. Xie, Phys. Rev. D **87** (2013) no.9, 096006 doi:10.1103/PhysRevD.87.096006 [arXiv:1304.1021 [hep-ph]].
- [12] F. E. Close and Q. Zhao, Phys. Rev. D **71** (2005), 094022 doi:10.1103/PhysRevD.71.094022 [arXiv:hep-ph/0504043 [hep-ph]].
- [13] L. C. Gui *et al.* [CLQCD], Phys. Rev. Lett. **110**, 021601 (2013). doi:10.1103/PhysRevLett.110.021601 [arXiv:1206.0125 [hep-lat]].
- [14] S. Janowski, F. Giacosa and D. H. Rischke, Phys. Rev. D **90**, 114005 (2014). doi:10.1103/PhysRevD.90.114005 [arXiv:1408.4921 [hep-ph]].
- [15] A. H. Fariborz, A. Azizi and A. Asrar, Proximity of  $f_0(1500)$  and  $f_0(1710)$  to the scalar glueball, Phys. Rev. D **92**, 113003 (2015).
- [16] Y. Chen, A. Alexandru, S. J. Dong, T. Draper, I. Horvath, F. X. Lee, K. F. Liu, N. Mathur, C. Morningstar and M. Peardon, *et al.* Phys. Rev. D **73** (2006), 014516 doi:10.1103/PhysRevD.73.014516 [arXiv:hep-lat/0510074 [hep-lat]].
- [17] L. S. Geng and E. Oset, Phys. Rev. D **79** (2009), 074009 doi:10.1103/PhysRevD.79.074009 [arXiv:0812.1199 [hep-ph]].
- [18] M. L. Du, D. Gülmez, F. K. Guo, U. G. Meißner and Q. Wang, Eur. Phys. J. C **78** (2018) no.12, 988 doi:10.1140/epjc/s10052-018-6475-8 [arXiv:1808.09664 [hep-ph]].
- [19] R. L. Workman *et al.* [Particle Data Group], PTEP **2022** (2022), 083C01 doi:10.1093/ptep/ptac097
- [20] Z. L. Wang and B. S. Zou, Eur. Phys. J. C **82** (2022) no.6, 509 doi:10.1140/epjc/s10052-022-10460-4 [arXiv:2203.02899 [hep-ph]].
- [21] G. Y. Wang, S. C. Xue, G. N. Li, E. Wang and D. M. Li, Phys. Rev. D **97** (2018) no.3, 034030 doi:10.1103/PhysRevD.97.034030 [arXiv:1712.10180 [hep-ph]].
- [22] Q. H. Shen, X. Zhang, X. Liu and J. J. Xie, Phys. Rev. D **109** (2024) no.1, 014012 doi:10.1103/PhysRevD.109.014012 [arXiv:2310.07258 [hep-ph]].
- [23] D. Guo, W. Chen, H. X. Chen, X. Liu and S. L. Zhu, Phys. Rev. D **105** (2022) no.11, 114014 doi:10.1103/PhysRevD.105.114014 [arXiv:2204.13092 [hep-ph]].
- [24] M. Ablikim *et al.* [BES], Phys. Rev. Lett. **96** (2006), 162002 doi:10.1103/PhysRevLett.96.162002 [arXiv:hep-ex/0602031 [hep-ex]].
- [25] M. Ablikim *et al.* [BESIII], Phys. Rev. D **87** (2013) no.3, 032008 doi:10.1103/PhysRevD.87.032008 [arXiv:1211.5668 [hep-ex]].
- [26] X. Zhu, D. M. Li, E. Wang, L. S. Geng and J. J. Xie, Phys. Rev. D **105** (2022) no.11, 116010 doi:10.1103/PhysRevD.105.116010 [arXiv:2204.09384 [hep-ph]].
- [27] X. Zhu, H. N. Wang, D. M. Li, E. Wang, L. S. Geng and J. J. Xie, Phys. Rev. D **107** (2023) no.3, 034001 doi:10.1103/PhysRevD.107.034001 [arXiv:2210.12992 [hep-ph]].
- [28] L. R. Dai, E. Oset and L. S. Geng, Eur. Phys. J. C **82** (2022) no.3, 225 doi:10.1140/epjc/s10052-022-10178-3 [arXiv:2111.10230 [hep-ph]].
- [29] E. Oset, L. R. Dai and L. S. Geng, Sci. Bull. **68** (2023), 243-246 doi:10.1016/j.scib.2023.01.011 [arXiv:2301.08532 [hep-ph]].
- [30] Z. Y. Wang, Y. W. Peng, J. Y. Yi, W. C. Luo and C. W. Xiao, Phys. Rev. D **107** (2023) no.11, 116018 doi:10.1103/PhysRevD.107.116018
- [31] Y. Ding, X. H. Zhang, M. Y. Dai, E. Wang, D. M. Li, L. S. Geng and J. J. Xie, Phys. Rev. D **108**, no.11, 114004 (2023) doi:10.1103/PhysRevD.108.114004 [arXiv:2306.15964 [hep-ph]].
- [32] J. P. Lees *et al.* [BaBar], Phys. Rev. D **93** (2016), 012005 doi:10.1103/PhysRevD.93.012005 [arXiv:1511.02310 [hep-ex]].
- [33] X. Y. Wang, H. F. Zhou and X. Liu, Phys. Rev. D **108** (2023) no.3, 034015 doi:10.1103/PhysRevD.108.034015 [arXiv:2306.12815 [hep-ph]].
- [34] M. Ablikim *et al.* [BESIII], Chin. Phys. C **46** (2022) no.7, 074001 doi:10.1088/1674-1137/ac5c2e [arXiv:2111.07571 [hep-ex]].
- [35] M. Achasov, X. C. Ai, L. P. An, R. Aliberti, Q. An, X. Z. Bai, Y. Bai, O. Bakina, A. Barnyakov and V. Blinov, *et al.* Front. Phys. (Beijing) **19** (2024) no.1, 14701 doi:10.1007/s11467-023-1333-z [arXiv:2303.15790 [hep-ex]].
- [36] J. P. Lees *et al.* [BaBar], Phys. Rev. D **95** (2017) no.9, 092005 doi:10.1103/PhysRevD.95.092005 [arXiv:1704.05009 [hep-ex]].
- [37] L. S. Geng, E. Oset, L. Roca and J. A. Oller, Phys. Rev. D **75** (2007), 014017 doi:10.1103/PhysRevD.75.014017 [arXiv:hep-ph/0610217 [hep-ph]].
- [38] G. Y. Wang, L. Roca, E. Wang, W. H. Liang and E. Oset, Eur. Phys. J. C **80** (2020) no.5, 388 doi:10.1140/epjc/s10052-020-7939-1 [arXiv:2002.07610 [hep-ph]].
- [39] G. Y. Wang, L. Roca and E. Oset, Phys. Rev. D **100** (2019) no.7, 074018 doi:10.1103/PhysRevD.100.074018 [arXiv:1907.09188 [hep-ph]].
- [40] J. M. Xie, J. X. Lu, L. S. Geng and B. S. Zou, [arXiv:2312.17287 [hep-ph]].
- [41] J. M. Xie, J. X. Lu, L. S. Geng and B. S. Zou, Phys. Rev. D **108** (2023) no.11, L111502

- doi:10.1103/PhysRevD.108.L111502 [arXiv:2307.11631 [hep-ph]].
- [42] N. Ikeno, J. M. Dias, W. H. Liang and E. Oset, Phys. Rev. D **100** (2019) no.11, 114011 doi:10.1103/PhysRevD.100.114011 [arXiv:1909.11906 [hep-ph]].
- [43] S. J. Jiang, S. Sakai, W. H. Liang and E. Oset, Phys. Lett. B **797** (2019), 134831 doi:10.1016/j.physletb.2019.134831 [arXiv:1904.08271 [hep-ph]].
- [44] S. Sakai, W. H. Liang, G. Toledo and E. Oset, Phys. Rev. D **101** (2020) no.1, 014005 doi:10.1103/PhysRevD.101.014005 [arXiv:1909.08888 [hep-ph]].
- [45] H. Zhang, B. C. Ke, Y. Yu and E. Wang, Chin. Phys. C **47** (2023) no.6, 063101 doi:10.1088/1674-1137/acc642 [arXiv:2302.10541 [hep-ph]].
- [46] J. Y. Wang, M. Y. Duan, G. Y. Wang, D. M. Li, L. J. Liu and E. Wang, Phys. Lett. B **821** (2021), 136617 doi:10.1016/j.physletb.2021.136617 [arXiv:2105.04907 [hep-ph]].
- [47] M. Y. Duan, G. Y. Wang, E. Wang, D. M. Li and D. Y. Chen, Phys. Rev. D **104** (2021) no.7, 074030 doi:10.1103/PhysRevD.104.074030 [arXiv:2109.00731 [hep-ph]].
- [48] L. M. Abreu, W. F. Wang and E. Oset, Eur. Phys. J. C **83** (2023) no.3, 243 doi:10.1140/epjc/s10052-023-11384-3 [arXiv:2301.08058 [hep-ph]].
- [49] R. Molina, L. R. Dai, L. S. Geng and E. Oset, Eur. Phys. J. A **56** (2020) no.6, 173 doi:10.1140/epja/s10050-020-00176-y [arXiv:1909.10764 [hep-ph]].
- [50] R. Molina, D. Nicmorus and E. Oset, Phys. Rev. D **78** (2008), 114018 doi:10.1103/PhysRevD.78.114018 [arXiv:0809.2233 [hep-ph]].
- [51] W. T. Lyu, Y. H. Lyu, M. Y. Duan, D. M. Li, D. Y. Chen and E. Wang, Phys. Rev. D **109** (2024) no.1, 014008 doi:10.1103/PhysRevD.109.014008 [arXiv:2306.16101 [hep-ph]].
- [52] M. Y. Duan, D. Y. Chen and E. Wang, Eur. Phys. J. C **82** (2022) no.10, 968 doi:10.1140/epjc/s10052-022-10948-z [arXiv:2207.03930 [hep-ph]].
- [53] L. S. Geng, E. Oset, R. Molina and D. Nicmorus, PoS **EFT09** (2009), 040 doi:10.22323/1.069.0040 [arXiv:0905.0419 [hep-ph]].